

Room-Temperature Ordered Photon Emission from Multiexciton States in Single CdSe Core-Shell Nanocrystals

Brent Fisher,¹ Jean Michel Caruge,¹ Don Zehnder,² and Mounji Bawendi¹

¹*Department of Chemistry, Massachusetts Institute of Technology, 77 Massachusetts Avenue, Cambridge, Massachusetts 02139, USA*

²*Quantum Dot Corp., 26118 Research Road, Hayward, California 94545, USA*

(Received 31 August 2004; published 3 March 2005)

We report room-temperature ordered multiphoton emission from multiexciton states of *single* CdSe(CdZnS) core(-shell) colloidal nanocrystals (NCs) that are synthesized by wet chemical methods. Spectrally and temporally resolved measurements of biexciton and triexciton emission from single NCs are also presented. A simple four level system models the results accurately and provides estimates for biexciton and triexciton radiative lifetimes and quantum yields.

DOI: 10.1103/PhysRevLett.94.087403

PACS numbers: 78.67.Bf, 42.50.-p, 78.47.+p, 79.60.Jv

Sources of nonclassical light and ordered multiphoton emission offer a fascinating example of the quantum nature of light and have received attention because of their potential use in quantum cryptography [1,2]. The first sources of nonclassical radiation were isolated atoms [3,4], ions [5], or molecules [6]. However, single semiconductor quantum dots (QDs) have recently proven capable of providing highly efficient sources of sub-Poissonian or antibunched light [7,8], triggered single photons [9], correlated photon pairs [10–12], and even three stage radiative quantum cascades [13]. Single QDs have even enabled the generation of entangled photon pairs [14]. The QDs used in these previous experiments were fabricated using Stranski-Krastanov growth or similar self-assembly methods in highly controlled vacuum conditions, and have typically been InAs or InP QDs [13,15].

Colloidal semiconductor nanocrystals (NCs) are related to QDs but are distinct. Instead of vacuum deposition techniques, NCs are synthesized by wet chemical methods in organic colloidal suspensions with good size and shape control. NCs are typically smaller and more spherically symmetric than QDs, which can lead to stronger carrier confinement. The low cost and processing versatility of NCs have already led to commercial applications in biological labeling, while other applications ranging from lasing [16,17] to light emitting diodes [18] have been demonstrated. The use of single NCs for nonclassical light generation was only recently investigated when antibunching from CdSe(ZnS) core-shell NCs was reported [19–21]. There have been, however, no reports of ordered multiphoton generation using NCs. This is because Auger relaxation in NCs can quench multiexciton emission within a few picoseconds leading to negligible multiexciton quantum yields (QYs) [22].

Despite strong Auger relaxation in NCs, two recent reports have shown multiexciton photoluminescence (PL) from ensembles of NCs using transient detection techniques [23,24]. In the work of Ref. [23] CdSe(ZnS) core(-shell) NCs exhibited both biexciton (BX) and triexciton (TX) emission with the TX blueshifted 100–

250 meV from the single exciton (X) depending on NC size.

In this Letter, we report spectrally and temporally resolved multiexciton emission from single CdSe(CdZnS) core(-shell) NCs prepared by wet chemical synthesis. Furthermore, we show for single NCs that ordered photon emission occurs in a cascade from multiexciton states. A simple four level system (4LS) model reproduces the results and gives estimates for the QYs and radiative lifetimes of the BX and TX.

We used high QY (30%–80%) CdSe(CdZnS) core(-shell) NCs of various sizes (2.5–5 nm, core radius) synthesized in our laboratory or obtained from Quantum Dot Corp. (QDC), (Catalog No. 1002-1). The data presented in this Letter were taken from the QDC sample (radius 5.1 nm, 655 nm PL band, 75% QY), although similar results were obtained from all large samples (~5 nm radius). Transient spectra from NC solutions were obtained on a streak camera (Hamamatsu) after excitation at 400 nm by a frequency-doubled, amplified Ti:sapphire laser (1 kHz). For single NC experiments a dilute solution of the NCs was spin coated onto a cover glass to produce a low-density field of single NCs ($< 0.1 \mu\text{m}^{-2}$). Single NCs were excited using either a continuous wave Ar⁺ laser at 514 nm or the 400 nm pulsed output of a frequency-doubled Ti:sapphire oscillator ($\tau_{\text{pulse}} < 500$ fs, 4.715 MHz repetition rate). PL from single NCs was collected on a home-built scanning confocal microscope. A Timeharp200 (Picoquant) was used to perform time correlated single photon counting (TCSPC) on single NCs, which yielded lifetimes or single photon coincidence histograms, $n(\tau)$, when detecting PL in the Hanbury-Brown–Twiss (HBT) geometry (50/50 nonpolarizing beam splitter). Transient spectra of single NCs were obtained using an ultrafast, gated charged coupled device (LaVision GmbH). All measurements were at room temperature (RT).

Figure 1 presents streak camera measurements of a solution of NCs revealing clear multiexciton features. Plot (a) shows transient PL spectra for high intensity

excitation ($\nu = 6$ excitons/NC/pulse) at progressively longer delays. The blueshifted emission originates from the TX and is separated by about 140 meV, in agreement Ref. [23]. The main peak contains both X and BX emission (denoted X + BX) since the redshift of the BX is less than the ensemble emission linewidth at RT.

Figure 1(b) presents the temporal profiles of both the TX and X + BX emission bands for low and high excitation intensity. By comparing the integrated area of the pure BX decay component to the area of the pure X decay, we can estimate the QY of the BX (Q_2) relative to that of the X (Q_1): $q_2 = Q_2/Q_1 = 0.11$. An analogous calculation for the TX yields $q_3 = Q_3/Q_1 = 0.05$.

Figure 1(c) plots the subnanosecond lifetimes of the BX and TX on a log scale with corresponding fits. The BX decay component was obtained by subtracting the “background” intensity at 4.2 ns from the X + BX curve—long after the BX has decayed. These lifetimes are much longer than previously reported Auger lifetimes [22] (which used smaller NCs than here), and they support the large q_2 and q_3 values obtained above. Extending the linear dependence of the Auger recombination time on NC volume (Ref. [22])

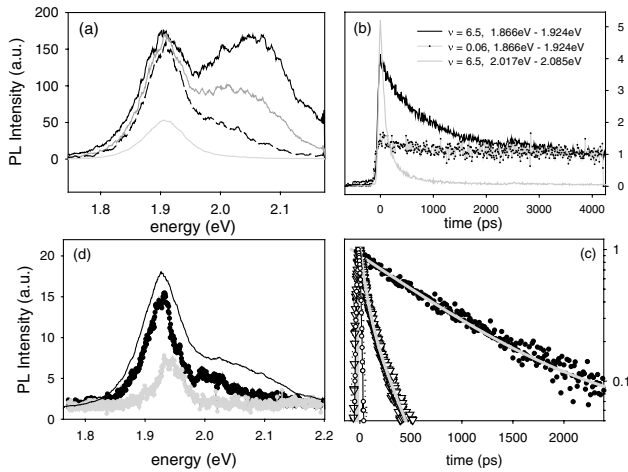


FIG. 1. (a) Transient spectra of a NC solution for various delay ranges: -50 – 50 ps; 50 – 150 ps; 250 – 350 ps; 3 – 4 ns. (b) PL decays obtained from X + BX and TX regions of transient spectra, 1.87 – 1.92 eV and 2.02 – 2.09 eV, respectively, at low ($2 \mu\text{J}/\text{cm}^2$) and high ($240 \mu\text{J}/\text{cm}^2$) fluence. Data are rescaled so that low and high intensity X + BX decays match at 4.2 ns. The integrated areas of pure TX, BX, and X decay components, taken with the initial excitation probability (p_i^o) and PL bandwidth ($\Delta\lambda$) of each state, allow calculation of relative QYs (Q_i/Q_1): $\frac{A_{\text{BX,TX}}}{A_X} \frac{\Delta\lambda_{\text{BX,TX}}}{\Delta\lambda_X} \approx \frac{\text{BX,TX counts}}{\text{X counts}} = \frac{Q_{2,3} \times p_{2,3}^o}{Q_1 \times p_{\leq 1}^o}$ (c) Log-scaled lifetimes of BX (\bullet) and TX (∇) with instrument response (\circ) and exponential fits (BX: $1/\Gamma_2 = 790$ ps; TX: $1/\Gamma_3 = 230$ ps—slow component of bi-exponential fit). (d) Transient spectra (1000 ps gate) from a single NC ($280 \mu\text{J}/\text{cm}^2$) at 0 (\bullet) and 5 ns (gray circle) delay. The ensemble transient spectrum (solid line) from (a) is superimposed (1000 ps integrated, 10 meV shift for comparison).

to our larger NCs (5.1 nm radius) yields a biexciton lifetime of 714 ps, in agreement with our measurement. These long lifetimes and high QYs are critical to our subsequent detection of multiexciton emission and ordered multiphoton emission in single NCs.

Figure 1(d) shows two transient (1000 ps time-gated) emission spectra from a single NC, taken at different post-excitation delays. The zero-delay spectrum integrates over the lifetime of the TX, revealing blueshifted TX emission from the single NC, which is in qualitative agreement with the transient spectrum of the solution (black line). In contrast, the single NC spectrum obtained after a 5 ns delay (gray line) shows no blueshifted emission band, because the TX has completely decayed. The single NC spectrum at 5 ns delay does not coincide with the main peak at zero delay because of spectral diffusion.

Observation of multiexciton emission in the spectra of single NCs implies that its signature should be evident in the spectrally integrated lifetime of single NCs as well. Figure 2(a) presents a series of lifetime measurements of the same single NC taken at different excitation intensities. All decays show a slow component (29 ns ± 1 ns), but as the intensity is increased, a fast component appears (instrument limited, ~ 1 ns) that originates from spectrally observed BX and TX emission. Figure 2(b) plots the intensity dependence of the fast component, expressed as the ratio of fast and slow weighting parameters obtained from biexponential fits of the lifetimes. For pulsed experiments the time evolution of the occupation probabilities [$p_i(t)$] in the 4LS after pulsed excitation is given by ($\tau_{\text{pulse}} \ll 1/\Gamma_i$)

$$\begin{aligned} \frac{dp_3(t)}{dt} &= -\Gamma_3 p_3(t), & \frac{dp_2(t)}{dt} &= \Gamma_3 p_3(t) - \Gamma_2 p_2(t), \\ \frac{dp_1(t)}{dt} &= \Gamma_2 p_2(t) - \Gamma_1 p_1(t). \end{aligned} \quad (1)$$

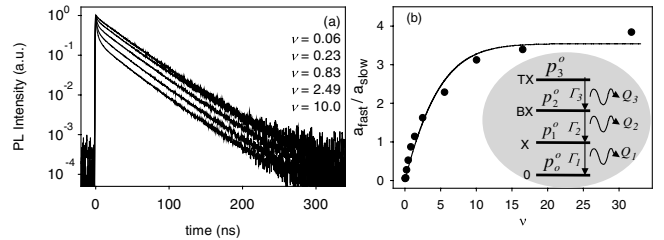


FIG. 2. (a) Spectrally integrated lifetimes of a single NC at various excitation intensities ($P_o = 4 \mu\text{J}/\text{cm}^2$). (b) Dots: intensity dependence of the biexponential weighting components, a_{fast} and a_{slow} , from fits to the lifetimes. Line: best fit of the data to Eq. (2), which yielded $q_2 = 0.14$ and $q_3 = 0.04$. Illustration: graphical description of 4LS model. $\Gamma_1, \Gamma_2, \Gamma_3$ are relaxation rates and Q_1, Q_2, Q_3 radiative QYs of X, BX, and TX, respectively. p_i^o 's are initial conditions given by the Poisson distributed probability of exciting 0, 1, 2, >2 excitons in a NC, given an average number of excitons generated per pulse, ν .

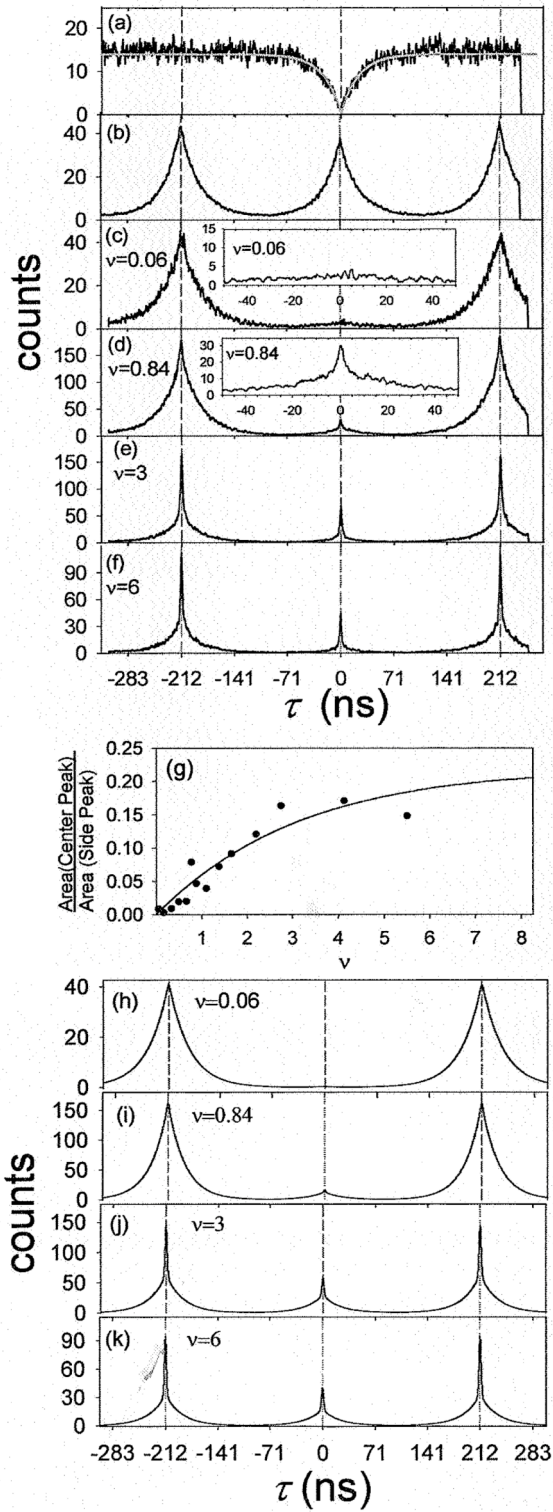


FIG. 3. (a) $n(\tau)$ for a single NC under cw excitation (60 W/cm^2). $n(\tau = 0)/n(\infty) < 0.05$; an exponential fit (gray line) gives $n(0)/n(\infty) = 0.025$. (b) $n(\tau)$ for a collection of NCs under low-intensity, pulsed excitation. (c)–(f) Same as (b) but from a *single* NC under various excitation intensities. (g) Ratio of center to side peak area versus excitation intensity (\bullet) along with the calculated value (solid line). (h)–(k) Calculated $n(\tau)$ for experiments (c)–(f).

Solutions of Eq. (1) give the time dependence of the total PL, $\text{PL}(t) = \sum_{i=1}^3 Q_i \Gamma_i p_i(t)$, where $p_i(t)$ are obtained using standard methods. Since the TCSPC response was slower than the first two components of the total PL decay, these fast terms are combined into a single response-limited component. This yields a *two-component* total PL decay, $\text{PL}(t) = a_{\text{fast}} e^{-\Gamma_{\text{fast}} t} + a_{\text{slow}} e^{-\Gamma_{\text{slow}} t}$, which leads to an expression for the intensity dependence of the data in Fig. 2(b):

$$\frac{a_{\text{fast}}}{a_{\text{slow}}} = \frac{q_3 \eta_3 p_3^0 + (q_2 \eta_2 - 1) p_2^0}{p_1^0 + p_2^0 + p_3^0}, \quad (2)$$

where $\eta_i = \Gamma_i/\Gamma_1$. Fixing the relaxation rates to measured values ($\Gamma_1 = 1/29 \text{ ns}$, $\Gamma_2 = 1/790 \text{ ps}$, $\Gamma_3 = 1/230 \text{ ps}$) and fitting Eq. (2) to the experimental data give $q_2 = 0.14$ and $q_3 = 0.04$ [best fit, Fig. 2(b)], in good agreement with the $q_2 = 0.11$ and $q_3 = 0.05$ obtained from Fig. 1(b). These values imply radiative lifetimes of 8.4 and 6.8 ns for the BX and TX, respectively.

With evidence of both spectrally and temporally resolved multiexciton emission from single colloidal NCs, the potential of this material for photon pair generation naturally comes to mind. Figure 3 presents RT HBT measurements of a single NC. Under low-intensity cw excitation, $n(\tau)$ shows the strong antibunching [Fig. 3(a)] previously reported [19,20], confirming that the photon sources probed were truly single NCs.

Figures 3(b) and 3(c) display $n(\tau)$ obtained using pulsed excitation of *many* NCs [3(b)] and of a *single* NC [3(c)]. Since normalization of $n(\tau)$ to the second order correlation function, $g^{(2)}(\tau)$, cannot be easily obtained in pulsed HBT experiments, $n(\tau)$ is presented without normalization. In the experiment of 3(b), a collection of NCs was excited by each pulse so the possibility of detecting >1 photon after a single excitation pulse is not suppressed, and a peak appears at $\tau = 0$. $n(\tau)$ from a single NC [3(c)], on the other hand, is missing the peak at $\tau = 0$ because emission of a photon projects the NC into the ground state so that one and only one photon can be emitted per excitation pulse (low-intensity excitation ensured that $\nu < 1$). If every pulse were to excite the NC, this would be an optically driven single photon turnstile device operating at room temperature.

As the excitation intensity is raised, however [Figs. 3(d)–3(f), *same* NC], a symmetric center peak appears in $n(\tau)$, indicating that multiple photons are emitted from the single NC after excitation by a single laser pulse. Multiple photons originate from emission out of the X plus the BX and/or TX states of the single NC, which can be accessed only by higher intensity excitation pulses.

The intensity dependence of the multiphoton emission was quantified in Fig. 3(g) by the ratio of the areas (measured by fitting) of the center and side peaks in $n(\tau)$ from the same single NC. The ratio of areas was used as a normalization to account for differences in collection

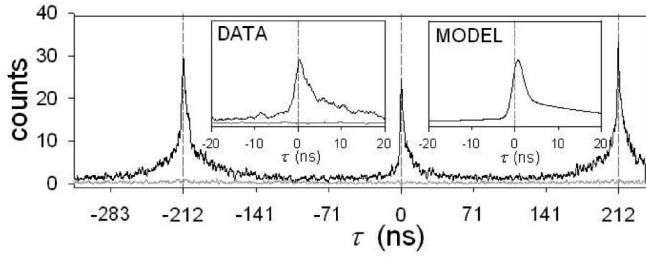


FIG. 4. Black line: $n(\tau)$ for asymmetric HBT experiment at high excitation fluence ($120 \mu\text{J}/\text{cm}^2$). Gray line: $n(\tau)$ at low excitation fluence ($< 20 \mu\text{J}/\text{cm}^2$) using same setup. Left inset: close up of $n(\tau)$. Right Inset: $n(\tau)$ predicted by the 4LS for a single NC under high intensity excitation. Vertical cursors: laser repetition rate.

time, coincidence rate, etc. Solutions of the 4LS were used to model $n(\tau)$ at different excitation intensities and to predict the intensity dependence of the center peak based on the values of Γ_i and q_i determined earlier. Temporal profiles, $R_i(t)$, of emission from the multiexciton states were calculated by multiplying the solutions of Eq. (1) by the corresponding radiative relaxation rates ($k_i = Q_i\Gamma_i$). The second order correlation function was then calculated for each type of photon coincidence event (e.g., X and BX or X and X):

$$g_{i,j}^{(2)}(\tau) = \frac{\langle R_i(t)R_j(t+\tau) \rangle}{\langle R_i(t) \rangle \langle R_j(t+\tau) \rangle} - 1, \quad (3)$$

where the angular brackets indicate time averaging, and $i, j = (1, 2, 3)$ indicate (X, BX, TX). Finally, the total $g^{(2)}(\tau)$ was obtained by a weighted average,

$$g_{\text{tot}}^{(2)}(\tau) = \frac{\sum_{i,j=1}^3 \langle R_i \rangle \langle R_j \rangle g_{i,j}^{(2)}(\tau)}{\langle R_1 + R_2 + R_3 \rangle^2}. \quad (4)$$

Equations (3) and (4) allow modeling of the excitation intensity dependence of the center versus side peak area ratio in Fig. 3(g), which is superimposed as a solid line on the actual data with good agreement. In Figs. 3(h)–3(k) the predicted $g^{(2)}(\tau)$ is plotted for the same intensities used in experiments [$g^{(2)}(\tau)$ is rescaled to match $n(\tau)$ at each intensity]. A blinking induced reduction of Q_1 , experimentally observed at high excitation intensities, was included for modeling the curves at high intensity. Given the simplicity of the model, the predicted plots for $g^{(2)}(\tau)$ show a strong similarity to those obtained experimentally.

Figure 4 gives the most conclusive evidence of ordered multiphoton emission from single NCs. A narrow band pass filter (2.015–2.045 eV) in front of the start detector, and a long pass filter (1.97 eV cutoff) in front of the stop detector, restricts TX photons to the start detector and BX and X photons to the stop detector only. Practically no coincidence events are observed at low intensity, since the TX is not generated. At high intensity, however, an *asym-*

metric center peak is obtained. The asymmetry is observed because TX photons necessarily precede BX and X photons—the photon emission is ordered. These data are reproduced by the 4LS model (right inset).

The emergence of a center peak at higher intensities in $n(\tau)$ of Fig. 3, along with the asymmetry of the center peak in Fig. 4, demonstrates ordered photon emission from multiexciton states of single NCs. This constitutes a significant advance in the study of the optical properties of colloidal NCs. Auger relaxation has been considered an unavoidable characteristic of NCs and has prevented observation of multiexcitonic states, causing NCs to be neglected as a viable source for photon pair production. These results show that, in fact, large NCs can produce ordered multiphoton emission, even at RT. The long-term photostability of single NCs is also an obstacle to their practical implementation as a single or photon pair source at room temperature. The samples investigated still exhibited blinking and often photobleached after many minutes of high intensity excitation. Nevertheless, in light of the fact that we can now observe multiexciton emission from NCs—a previously disregarded possibility because of Auger relaxation—we are optimistic that continued rapid development of NC chemistry and processing can circumvent blinking and allow NCs to serve as practical sources of controlled single and ordered multiphoton emission.

This work was supported by the Center for Materials Science (DMR-0213282) and the Department of Energy (DE-FG02-02ER45974). We are grateful to Justin Hodgkiss for streak camera assistance, and Xavier Brokmann for discussions.

-
- [1] N. Gisin *et al.*, Rev. Mod. Phys. **74**, 145 (2002).
 - [2] G. Brassard *et al.*, Phys. Rev. Lett. **85**, 1330 (2000).
 - [3] H.J. Kimble *et al.*, Phys. Rev. Lett. **39**, 691 (1977).
 - [4] R. Short and L. Mandel, Phys. Rev. Lett. **51**, 384 (1983).
 - [5] F. Diedrich *et al.*, Phys. Rev. Lett. **58**, 203 (1987).
 - [6] T. Basche *et al.*, Phys. Rev. Lett. **69**, 1516 (1992).
 - [7] C. Becher *et al.*, Phys. Rev. B **63**, 121312 (2001).
 - [8] V. Zwiller *et al.*, Appl. Phys. Lett. **78**, 2476 (2001).
 - [9] C. Santori *et al.*, Phys. Rev. Lett. **86**, 1502 (2001).
 - [10] A. Kiraz *et al.*, Phys. Rev. B **65**, 161303 (2002).
 - [11] E. Moreau *et al.*, Phys. Rev. Lett. **87**, 183601 (2001).
 - [12] C. Santori *et al.*, Phys. Rev. B **66**, 045308 (2002).
 - [13] J. Persson *et al.*, Phys. Rev. B **69**, 233314 (2004).
 - [14] D. Fattal *et al.*, Phys. Rev. Lett. **92**, 037903 (2004).
 - [15] V. Zwiller *et al.*, Appl. Phys. Lett. **82**, 1509 (2003).
 - [16] H.J. Eisler *et al.*, Appl. Phys. Lett. **80**, 4614 (2002).
 - [17] V.I. Klimov *et al.*, Science **290**, 314 (2000).
 - [18] S. Coe *et al.*, Nature (London) **420**, 800 (2002).
 - [19] B. Lounis *et al.*, Chem. Phys. Lett. **329**, 399 (2000).
 - [20] P. Michler *et al.*, Nature (London) **406**, 968 (2000).
 - [21] X. Brokmann *et al.*, Appl. Phys. Lett. **85**, 712 (2004).
 - [22] V.I. Klimov *et al.*, Science **287**, 1011 (2000).
 - [23] J.M. Caruge *et al.*, Phys. Rev. B **70**, 085316 (2004).
 - [24] M. Achermann *et al.*, Phys. Rev. B **68**, 245302 (2003).